

Ultrafast Raman-induced Kerr-effect of water: Single molecule versus collective motions

Kathrin Winkler, Jörg Lindner, Helge Bürsing, and Peter Vöhringer

Citation: *The Journal of Chemical Physics* **113**, 4674 (2000); doi: 10.1063/1.1288690

View online: <http://dx.doi.org/10.1063/1.1288690>

View Table of Contents: <http://scitation.aip.org/content/aip/journal/jcp/113/11?ver=pdfcov>

Published by the [AIP Publishing](#)

Articles you may be interested in

[Low-frequency collective dynamics in deep eutectic solvents of acetamide and electrolytes: A femtosecond Raman-induced Kerr effect spectroscopic study](#)

J. Chem. Phys. **141**, 134506 (2014); 10.1063/1.4897207

[Temperature- and solvation-dependent dynamics of liquid sulfur dioxide studied through the ultrafast optical Kerr effect](#)

J. Chem. Phys. **124**, 024506 (2006); 10.1063/1.2145760

[A new ultrafast technique for measuring the terahertz dynamics of chiral molecules: The theory of optical heterodyne-detected Raman-induced Kerr optical activity](#)

J. Chem. Phys. **122**, 244503 (2005); 10.1063/1.1937390

[Orientational and interaction induced dynamics in the isotropic phase of a liquid crystal: Polarization resolved ultrafast optical Kerr effect spectroscopy](#)

J. Chem. Phys. **120**, 10828 (2004); 10.1063/1.1737293

[The effects of anion and cation substitution on the ultrafast solvent dynamics of ionic liquids: A time-resolved optical Kerr-effect spectroscopic study](#)

J. Chem. Phys. **119**, 464 (2003); 10.1063/1.1578056



AIP | APL Photonics

APL Photonics is pleased to announce
Benjamin Eggleton as its Editor-in-Chief



Ultrafast Raman-induced Kerr-effect of water: Single molecule versus collective motions

Kathrin Winkler, Jörg Lindner, Helge Bürsing, and Peter Vöhringer^{a)}

Max-Planck-Institute for Biophysical Chemistry, Biomolecular and Chemical Dynamics Group, Am Faßberg 11, D-37077 Göttingen, Germany

(Received 3 May 2000; accepted 19 June 2000)

The ultrafast optical Kerr-response of water and heavy water has been measured at 1 bar in the temperature range between 273 and 373 K. The nuclear Kerr response of the liquid exhibits a pronounced double exponential decay on longer time scales after dephasing of impulsively perturbed acoustic modes is completed. The time constant, τ_2 , characterizing the slowly decaying exponential component of the Kerr-response function is in quantitative agreement with rotational diffusion time constants of the water molecules obtained from nuclear magnetic resonance (NMR) spin-lattice relaxation rates. A detailed comparison with THz time domain spectroscopy demonstrates that the reorientational dynamics responsible for the long time tail of the Kerr response are due to single molecule as opposed to collective effects. Furthermore, a good agreement between the single molecule rotational diffusion and the Stokes–Einstein–Debye equation is found in the temperature range of thermodynamic stability of the liquid. The time constant, τ_1 , characterizing the fast exponential component of the Kerr-response of water is found to be in qualitative agreement with central Lorentzian linewidths obtained from frequency-domain, depolarized Raman scattering experiments. The temperature dependence of τ_2 does not follow an Arrhenius-type behavior, which was previously taken as evidence for thermally activated crossing of a librational barrier with concomitant hydrogen-bond breakage. Instead, the temperature dependence of the fast relaxation time constant can be represented adequately by the Speedy–Angell relation which has been shown to accurately describe a number of transport parameters and thermodynamic properties of water. © 2000 American Institute of Physics. [S0021-9606(00)50635-7]

I. INTRODUCTION

The structure and the dynamics of water, the most abundant liquid on earth, has attracted an overwhelming interest of researchers for several centuries.¹ The tetrahedral coordination of water molecules through hydrogen bonding to nearest neighbors results in an unusually open random network structure which forms the basis of all peculiarities of this extraordinary liquid.² The probability of forming hydrogen-bonds increases with decreasing temperature thereby leading to a decreasing packing efficiency and a density maximum which is located at a temperature just above the melting temperature of ice. It was found that the density of the (metastable) supercooled liquid smoothly continues to follow the behavior observed in the stable liquid region, thus giving experimental access to a wider range of temperatures in which to study the anomalies of water.³

Besides the density, ρ , a number of other thermodynamic properties of water such as constant pressure heat capacity, C_p , isothermal compressibility, κ_T , or isobaric expansivity, α_p , show analogous anomalies as they tend to diverge upon approach of a singular temperature, T_S , located slightly below the homogeneous nucleation temperature, T_H , of the supercooled liquid.³ Singularities of these thermodynamic quantities suggest strongly increasing amplitudes of density, enthalpy, and entropy fluctuations in the liquid with decreasing

temperature, implying that the liquid becomes mechanically unstable in the vicinity of T_S .

Quite similarly, anomalies of dynamic transport parameters of water such as shear viscosity, η , inverse self diffusion coefficient, D^{-1} , or spin-lattice relaxation rates, R_1 , have been observed through careful studies over a wide range of pressure and temperature.^{3,4} These quantities offer information about the nature and the time scales of molecular motions in the liquid as they are described by time-correlation functions of dynamic variables. These, in turn, can be computed at a microscopic level through classical molecular-dynamics simulations.^{5–16}

Despite this tremendous amount of information compiled over many years of experimental and theoretical efforts, the anomalous behavior and its connection to structural ordering phenomena in the strongly hydrogen-bonded liquid network is as yet not fully understood. Thus, a detailed knowledge of structural relaxations on the time scale of hydrogen-bond motions is imperative in understanding the anomalous properties of this extraordinary liquid. Such knowledge will furthermore significantly improve our understanding of the role of this peculiar liquid in widespread areas of science ranging from climatology and regulatory mechanisms of our global weather to microbiology and structure-function relationships of proteins and nucleic acids.

Hence, experimental techniques are required which are sensitive to structural fluctuations directly on a time scale

^{a)}Electronic mail: pvoehri@gwdg.de

comparable to the lifetime of so-called intermittent V-type structures. These structures are nuclear conformations in the liquid which are averaged over the periods of typical intramolecular vibrations.² Vibrational spectroscopies such as infrared absorption or Raman scattering fulfill such requirements because the periods of intramolecular modes (10–100 fs) are short compared to the average time between diffusional jumps of molecules (1–10 ps). In addition, vibrational modes and their corresponding spectra are local probes of the environment of the molecules.

Of particular interest is light scattering activity in the so-called collision induced part of the Raman spectrum in the frequency range below 500 cm^{-1} . In this region, the underlying molecular degrees of freedom are believed to be directly correlated with hydrogen-bond motion.^{13,17–23} Two broad bands centered around 180 and 60 cm^{-1} originate from restricted translations parallel and perpendicular to intermolecular hydrogen bonds. Therefore, these modes closely effect stretching and bending motions of three hydrogen-bonded water molecules^{15,22} and arise principally from collision-induced effects dominated by long-range dipole-induced-dipole (DID) interaction.⁸ Beyond 300 cm^{-1} , the Raman spectrum reveals the optic modes of the liquid, i.e., the restricted rotational modes (or librations) about the three principal axes of inertia of the H_2O molecules.²¹ Finally, one or more central Lorentzian components are necessary to fully reproduce the low-frequency, depolarized Raman spectrum. However, various reports on these central components have yielded conflicting results as to their spectral distributions, their bandwidths and their physical nature due to an intrinsic overwhelming Rayleigh stray light level.^{17–20,24}

Nonresonant, Raman-induced optical Kerr-effect spectroscopy (OKE) with heterodyne detection (OHD-OKE) has been shown to be a full time-domain analogue of depolarized Raman scattering.²⁵ OHD-OKE has been applied before in numerous studies of the dynamics of neat liquids as well as binary mixtures.^{26–31} More interestingly, a few OHD-OKE studies have previously been published which focused on the nuclear dynamics in neat water.^{32–35} The intermolecular, restricted translational modes of the liquid gave rise to heavily damped coherent oscillations at their appropriate frequencies. Due to an insufficient time resolution, restricted rotational modes could be characterized only with very poor accuracy. Yet, with respect to long-time, exponential relaxation dynamics, complementary to the central Lorentzian components of the low-frequency Raman spectra, these OKE studies have also given contradictory results.^{32–35}

In this paper, we focus primarily on the temperature dependence of these long-time exponential relaxation dynamics since neither time nor frequency resolved Raman spectroscopies have so far been capable of providing a consistent and reliable picture for the corresponding underlying molecular motions in the liquid. In Sec. II, a brief description of our laser system and the Kerr-effect setup is given followed by a compilation of our experimental results in Sec. III. Section IV presents a detailed comparison with other spectroscopic probes of liquid dynamics in order to provide insights into the microscopic mechanisms responsible for the long

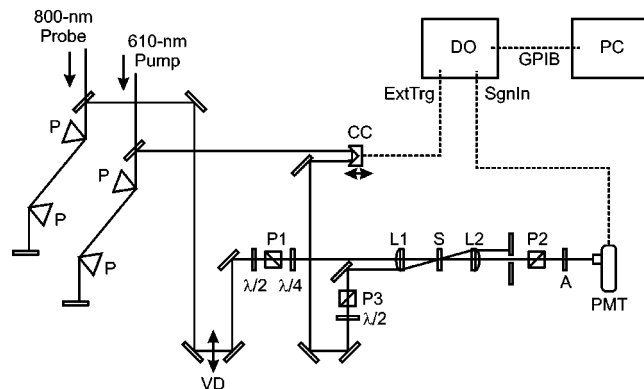


FIG. 1. Optical heterodyne-detected Kerr-effect arrangement. P: prisms for compensation of residual GVD. P1–P3: polarizers, CC: corner cube retroreflector, L1, L2: achromatic lenses, S: sample cell, $\lambda/2$: half-wave retardation plate, $\lambda/4$: quarter-wave retardation plate, VD: variable delay for time base calibration, DO: digital oscilloscope, PC: computer.

time exponential decays (or equivalently, central Raman Lorentzian components) observed in the ultrafast optical Kerr-effect of liquid water.

II. EXPERIMENT

OHD-OKE measurements were carried out with a Ti:sapphire laser/regenerative amplifier system capable of generating 800 nm, 30 fs optical pulses with energies as high as $4\ \mu\text{J}$ and repetition rates of 250 kHz. A portion (66%) of these amplified pulses were used to feed a collinearly pumped, white-light seeded optical parametric amplifier operating at a pump wavelength of 400 nm. Its output after compensation for group velocity dispersion (GVD) with a pair of LAFN_{28} prisms consisted of a 250 kHz train of transform-limited 30 fs pulses centered at 610 nm with energies as high as 200 nJ. Approximately 40 nJ of these pulses served as pump pulses in the Kerr-effect experiment. Probe pulses were derived with an uncoated fused silica substrate from the remaining 34% of the amplified 800 nm pulses. These pulses were also sent through a dispersive delay line to pre-compensate for any negative group velocity dispersion introduced by the Kerr-effect setup.

The Kerr-effect pump–probe arrangement is shown schematically in Fig. 1. After traveling through the prism pair arrangement, the 800 nm probe pulses were sent onto a computer controlled delay line (Melles Griot, Nanomover). The pulses were then directed through a combination of half-wave plate, Glan-Taylor polarizer (P1) and quarter-wave plate. Subsequently, the probe light was focused into the sample cell by an achromatic lens (L1) with a focal length of 100 mm. The half-wave plate allows for a fine adjustment of the probe energy at the sample whereas the quarter-wave plate allows for minimization of any residual static birefringence due to the lenses or the sample cell windows. Finally, the probe pulses were collimated by a second achromat ($f = 100\text{ mm}$) and directed through another Glan-Taylor polarizer onto a photomultiplier (Hamamatsu, 1P28). The polarizer, P2, is crossed with respect to P1 and provides an extinction ratio of at least 10^{-7} .

After GVD-(pre)compensation, the 610 nm pump pulses were sent into a rapid-scan delay line dithering sinusoidally at a frequency of 10 Hz with a maximum peak-to-peak displacement of 4 mm. The pump light then traveled through a combination of half-wave plate and Glan–Taylor polarizer (P3) before being spatially overlapped by L1 with the probe pulses at the location of the sample. The polarization of the pump was set to 45 degrees with respect to the polarization of the probe light.

The sample cell (Hellma, 160.001-OS, path length 1 mm) was carefully positioned in the probe beam path to minimize probe leakage through P2 due to static birefringence. Optical heterodyning was accomplished by slightly rotating P1, thereby providing an in-quadrature local oscillator field that is able to interfere with the signal field at the detector. The signal of the photomultiplier was directed through a fourth-order Butterworth filter with a 3 dB-cutoff frequency of 50 kHz. The filter had sufficient steepness to ensure that the optical Kerr-response on a real time scale of 1/10 s remained unperturbed. The output of the analog filter was then sent to a 16-bit digital oscilloscope (Tektronix, TDS 540) whose time base was triggered by an optical switch attached to the rapid scan delay line. The Kerr-effect signal could then be monitored and optimized in real time at a refresh rate of 10 Hz. The whole sampling depth of the oscilloscope was exploited, thus, giving 5000 A/D conversions (or equivalently, sampling points of the Kerr-transient) evenly distributed in a real time window of 20 ms. This time window proved sufficient to capture a pump–probe time delay window of about 14 ps.

The real-time base of the oscilloscope was calibrated prior to the experiment by recording a homodyne Kerr-response of a fused silica substrate with a thickness of 1 mm. The nanomover was stepped in increments of 20 fs and the peak position of such a signal was recorded while the rapid-scan stage was continuously dithered. The effect of stepping the nanomover by an independently known displacement was to shift the signal along the real-time axis of the oscilloscope.

It turned out that the heterodyne signal of the fused silica substrate is an excellent measure of the actual instrument response function, provided the sample cell windows are mimicked by an additional substrate of equal thickness and material (Hellma, OS) directly behind L1. For 1 mm of fused silica, the group delay difference between 800 and 610 nm is 34 fs. Furthermore, the group velocity dispersion in fused silica is such that a 610 nm light pulse after traveling through 1 mm of fused silica is broadened to ~ 95 fs whereas a 800 nm input pulse is lengthened to about 65 fs. The response function obtained in this manner had a full width at half maximum of 72 fs and agreed with the electronic (hyperpolarizability) contribution of independently measured Kerr-responses of numerous liquids that were measured in this setup.

Obviously, the major disadvantage of such a two-color Kerr-effect arrangement is a considerable loss of time resolution. However, pump and probe pulses are now spectrally separated which proved instrumental for liquids with very low Raman cross sections such as water. In fact, residual

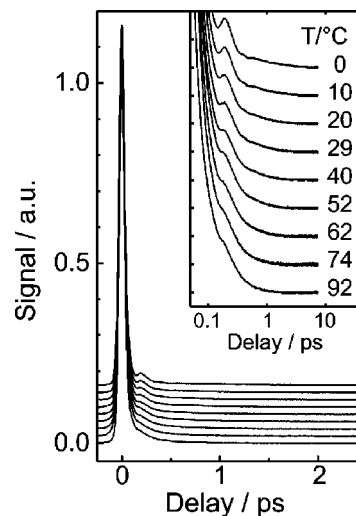


FIG. 2. Temperature dependent OHD-OKE transients of liquid water. The inset emphasizes the nuclear contribution to the Kerr response on a logarithmic delay scale.

pump stray light was substantially reduced in these experiments by employing an additional interference filter in front of the detector. The bandwidth of the spectral filter was matched to the spectral width of the probe pulses. A full heterodyne-detected Kerr-response was constructed from two independent measurements with local oscillator fields of equal amplitude but with opposite phases (i.e., $\pm \pi/2$). Each independent measurement itself consisted of an average of 600 individual scans and, therefore, required about 1 min of data acquisition time. A dynamic range of the full OHD-OKE transient, consisting of 5000 sampling points in a calibrated pump–probe delay window of 14 ps, of more than four decades was easily achieved by averaging for less than 10 min. The latter point clearly demonstrates the major advantage of this setup. As will be shown, a good signal-to-noise ratio was crucial to the experiments reported in the next section.³⁶

III. RESULTS

Representative, heterodyne-detected Kerr responses of water taken at different temperatures and at 1 atm are shown in Fig. 2. Around a pump–probe time delay of 0 ps, the signals are dominated by a strong spike which essentially follows the instrument response function. As described previously by McMorrow and Lotshaw, this instantaneous feature corresponds to the contribution of the electronic hyperpolarizability of the medium.²⁸ Although already present on the trailing edge of the zero-delay spike, nuclear contributions to the Kerr-response of water become more pronounced for significantly positive pump–probe time delays.

The most prominent nuclear contributions on short time scales are strongly damped coherent oscillations. As described extensively in Ref. 28, such oscillations arise from coherent superposition states of inter- and intramolecular modes of the liquid which are prepared through nonresonant Raman-transitions within the broad bandwidth of the pump-pulse. Since our emphasis is on the long time response of water, a detailed account on the temperature dependence of

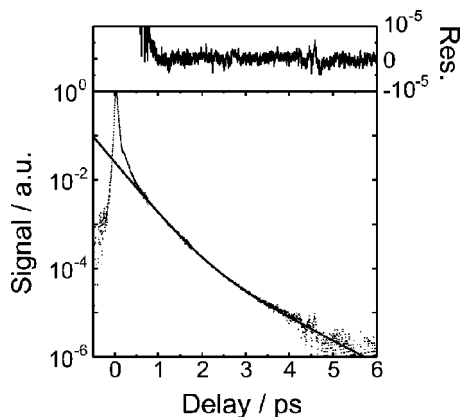


FIG. 3. Representative Kerr-effect transient at 347 K emphasizing the double exponential decay for longer delays. The upper panel displays the weighted residuals resulting from a bi-exponential fit to the data with time constants, $\tau_1=0.365$ ps and $\tau_2=0.85$ ps.

these features will be given elsewhere. Briefly, a detailed spectral analysis demonstrates that these oscillations essentially involve two broad Fourier components oscillating around 60 cm^{-1} and around 180 cm^{-1} . As already mentioned, these are precisely the hindered translational modes of liquid water which have been characterized in detail through low-frequency Raman scattering by Walrafen and co-workers.²¹ It turns out that the bandwidth of the high-frequency mode involving H-bond stretching increases with increasing temperature. Concurrently the same mode shifts to lower frequencies and gradually merges with the restricted translational mode at lower frequencies. As a result, the apparent damping of the oscillations in the time-domain Kerr-response increases with increasing temperature. This behavior can clearly be seen in the inset of Fig. 1 where the same data are plotted on a logarithmic time delay scale.

The same inset also emphasizes the long-time behavior of the data. It is evident that a slowly decaying nonoscillatory background contributes to the data which becomes faster as the temperature of the sample is raised. A semilogarithmic representation of the data taken at 347 K is shown in Fig. 3 which demonstrates that on longer time scales, the heterodyne-detected Kerr-response does not decay in a simple single exponential fashion. Instead, it was found that two exponential components are necessary to fully describe the long-time decay after dephasing of the impulsively driven acoustic modes is complete. The high quality of a fit according to a double exponential decay of the Kerr effect transient is demonstrated by the weighted residuals as shown in the upper panel of Fig. 3. The entire temperature dependence of the two time constants, τ_2 and τ_1 , characterizing the slow and the fast exponential component is summarized in Fig. 4.

IV. DISCUSSION

Multieponential tails in OKE measurements have been observed before in a number of chemically distinct nonhydrogen bonded molecular liquids.³¹ It is commonly believed that exponential decays at the longest delays arise exclusively from collective reorientation quantified by the second-

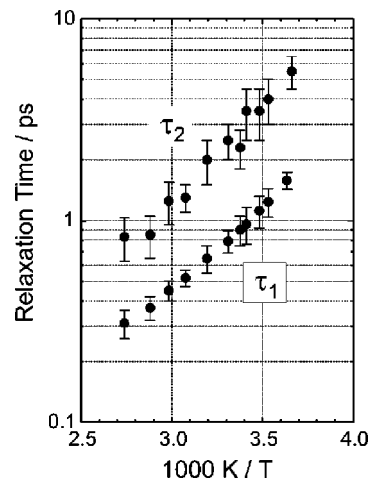


FIG. 4. Temperature dependence of the time constants characterizing the fast (τ_1) and slow (τ_2) exponential components to the nuclear Kerr response of water.

rank collective orientational correlation time.³¹ In general, removing this component leaves an additional exponential decay which has been termed the “intermediate response” whose origin is highly debated. According to an appealing interpretation given by Loughnane *et al.* these intermediate exponentials arise from structural relaxation dynamics in the motional narrowed regime.³¹ As shown in the previous section, the Kerr response of water does indeed show a double exponential decay on longer time scales and resembles very much the Kerr-response of nonassociating liquids. Therefore, one might be tempted to assign the slow time constant, τ_2 , to the collective orientational correlation time and the fast time constant, τ_1 , to the intermediate structural response as suggested in Ref. 31. However, it is highly instructive to compare our results with previous OKE studies and with other spectroscopic techniques which are also sensitive to reorientational dynamics in liquids.

A. Comparison with previous OHD-OKE data

The heterodyne-detected, nuclear Kerr-response of water has been measured previously by Castner and co-workers^{32,35} and by Palese *et al.*^{33,34} Similar to the data presented here, Castner *et al.* also report a bi-exponential decay on longer time scales which is characterized by time constants of 0.4 and 1.16 ps at room temperature. Based on a quantitative agreement with neutron scattering experiments, they attributed both components to rotational diffusion of the water molecules.

In contrast, temperature dependent OKE studies reported by Palese *et al.* revealed only a single exponential decay with a time constant of 600 fs at 298 K. Using amplified laser pulses and an in-phase local oscillator, however, the same authors were able to detect an additional exponential component with a time constant of 1.7 ps at room temperature. It was argued that the slower component originates from diffusive translational and rotational motions over larger length scales corresponding to dynamics of larger aggregates within the hydrogen-bonded liquid network structure. The faster component, on the other hand, was attributed

to orientational motion of small-size clusters or even individual molecules whose dynamics should be faster due to their smaller moment of inertia as compared to larger aggregates.

From our OHD-OKE data at room temperature, time constants of 0.9 and 2.5 ps can be extracted, clearly in contrast with these previous OKE studies. However, our slow time constant seems, at least qualitatively, similar to the slow time constant reported by Palese. On the other hand, our fast time constant seems to agree with the slow time constant reported by Castner *et al.* Indeed, after subtracting the double exponential fit with time constants, τ_1 and τ_2 , from the raw data, an artificial third exponential may be fitted to the tail of the residual, heavily damped acoustic modes whose time constant is found in the sub-500 fs region.

B. Comparison with NMR

According to a semiclassical description of ^1H nuclear magnetic resonance and under the assumption that proton translational and rotational motions are diffusive processes, the longitudinal, or equivalently the spin-lattice relaxation rate, R_1 , is proportional to the spectral density, $J(0)$, at zero frequency of the orientational correlation function.^{37–39}

$$G^{(2)} = \langle P_2[\mathbf{u}_j(0)\mathbf{u}_j(t)] \rangle. \quad (1)$$

Here $\mathbf{u}_j(t)$ is a unit vector in the molecule j and time t . The angular brackets denote canonical averages and P_2 is the Legendre polynomial of the order two. In order for Eq. (1) to be valid, the observable R_1 has to be corrected for intermolecular dipolar interactions caused by rotational motion of neighboring molecules.³⁷ Such corrected proton spin-lattice relaxation rates are, therefore, a direct measure of the single-molecule orientational correlation time, $\tau^{(2)}$

$$\tau^{(2)} = \int_0^\infty G^{(2)}(t) dt = J(0). \quad (2)$$

Spin-lattice relaxation rates of the nuclei D and ^{17}O , on the other hand, do not require any corrections for intermolecular dipolar interaction as they are entirely due to intramolecular quadrupolar interaction.^{38,39} Here, the inverse rate is directly linked to $G^{(2)}$ and $\tau^{(2)}$ as written in Eqs. (1) and (2). Lang and Lüdemann have reported detailed data for the pressure and temperature dependence of $\tau^{(2)}$ of water and heavy water using proton, deuteron, and 17 -oxygen longitudinal relaxation rates.^{4,37–39}

At pressures below 150 MPa, they found that the temperature dependence strictly obeyed the following equation:

$$\tau^{(2)} = \tau_S^{(2)} \left(\frac{T - T_S}{T_S} \right)^{-\gamma_S} \quad (3)$$

which was originally proposed by Speedy and Angell. Equation (3) has also been shown before to describe a number of static thermodynamic properties of liquid water extremely well.³ For light water, the singular temperature, T_S , at which the rotational correlation time apparently diverges was found to be 223 K at 1 atm with a corresponding critical exponent, γ_S , of 1.89. The frequency derived from the time constant ($\tau_S = 342$ fs at 1 atm) corresponds to restricted translational

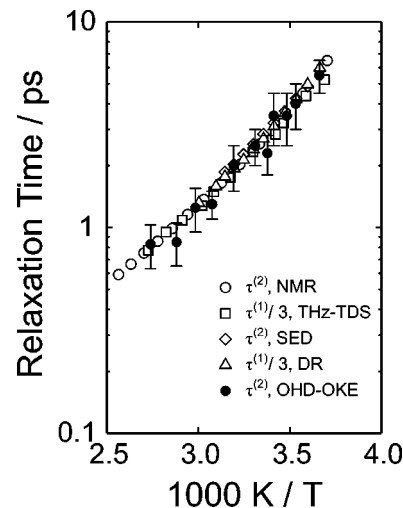


FIG. 5. Comparison of the time constant, τ_2 , characterizing the slow exponential component to the nuclear Kerr response of water (solid circles) with time constants obtained from other spectroscopic techniques. Open circles: single-molecule reorientational correlation times, $\tau^{(2)}$, calculated from experimental ^1H and ^{17}O spin lattice relaxation rates (from Refs. 4, 37–39). Squares: Debye relaxation times divided by three obtained in THz time domain spectroscopy (from Refs. 45 and 46). Diamonds: predictions of the Stokes–Einstein–Debye expression [Eq. (4)] using experimentally determined viscosities from Ref. 40. Triangles: dielectric relaxation times divided by three (Ref. 51).

motion perpendicular to intermolecular hydrogen bonds. This result was interpreted with fluctuations in the H-bond bending vibrations being the driving force of the anomalous density fluctuations upon approach of the mechanical stability limit of the liquid near T_S .^{4,39}

By comparing proton, deuteron, and 17 -oxygen longitudinal relaxation times, Lang and Lüdemann could furthermore demonstrate the isotropic nature of the single-molecule orientational correlation time.^{4,37–39}

The temperature dependence of $\tau^{(2)}$ according to Eq. (3) is compared in Fig. 5 to the temperature dependence of the slow exponential time constant, τ_2 , of our OHD-OKE transients. Due to the limited delay window of 14 ps, the scatter of our data is rather large. Yet, within our error, the agreement between these two different experimental techniques is quite surprising and strongly suggests that the slow exponential time constant observed here is identical to the single-molecule rather than the collective reorientational correlation time as previously suggested. In fact, a lack of convergence between NMR and previous OHD-OKE studies has led to the development of theoretical models which explains the long time exponential tail through nonlinear coupling of nuclear coordinates to the bulk liquid polarizability sensed by all time and frequency domain Raman spectroscopies.³³

Assuming for a moment that our slow exponential is indeed due to diffusive single-molecule reorientation, it is interesting to compare τ_2 with the classical Stokes–Einstein–Debye (SED) expression:

$$\tau^{(2)} = \frac{4\pi\eta a^3}{3k_B T}, \quad (4)$$

from standard hydrodynamic theory which works rather well for molecular, nonassociating liquids. Here, the rotating H_2O

molecule is assumed to have a spherical shape with a hydrodynamic radius $a=1.44 \text{ \AA}$ (see Ref. 2) and k_B is Boltzman's constant. Rotational correlation times calculated according to Eq. (4) are also included in Fig. 5. Surprisingly, we note that the SED predictions are quite accurate. Diffusive orientational motion of individual water molecules at 1 atm can apparently be described very well using a model that mimics the hydrogen-bonded liquid network by a viscous and structureless continuum. Since rotation of a water molecule involves the breakage and formation of hydrogen bonds to nearest neighbors, the success of the SED equation is indeed most surprising. Nevertheless, this agreement was already pointed out many years ago by Sposito.⁴⁰

C. Comparison with THz-TDS

Terahertz-time domain spectroscopy (THz-TDS) has recently become a powerful tool for exploring dynamics in neat liquids.^{41–47} In such experiments, the observable is the complex dielectric constant, $\epsilon(\omega)$, and therefore the index of refraction, $n(\omega)$, and the power absorption coefficient, $\alpha(\omega)$, in the frequency range between 0.1 and 2 THz. Keiding and co-workers have demonstrated that a double-Debye model is required to fully reproduce the line shape of $\epsilon(\omega)$ over the entire frequency interval accessible with the bandwidth of their THz pulses.^{45,46} A double Debye model is equivalent to a bi-exponential decay of the time correlation function

$$G^{(1)} = \left\langle P_1 \left[\mathbf{u}_i(0) \sum_j \boldsymbol{\mu}_j(t) \right] \right\rangle, \quad (5)$$

where $\boldsymbol{\mu}_i(t)$ is the dipole moment of the molecule i at time t and P_1 denotes the first-order Legendre polynomial. According to Eq. (5) and similar to an OHD-OKE experiment, THz-TDS is sensitive to collective dynamics. Neglecting the cross terms in Eq. (5) is equivalent to vanishing contributions from collective motions and the correlation function simplifies to

$$G^{(1)} = \langle P_1[\boldsymbol{\mu}_i(0)\boldsymbol{\mu}_i(0)] \rangle. \quad (6)$$

Now, the infinite time integral

$$\int_0^\infty G^{(1)}(t) dt = \tau^{(1)} \approx \tau_D, \quad (7)$$

can be approximated by the well-known Debye relaxation time, τ_D . As discussed by Lynden-Bell and Steele, if collective contributions are negligible, the following relation should hold:^{48–50}

$$\tau^{(2)} = \frac{\tau^{(1)}}{3} = \frac{\tau_D}{3}. \quad (8)$$

Keiding and co-workers also presented a detailed study of the temperature dependence of τ_D of liquid water at ambient pressure.^{45,46} Their data multiplied by a factor of 1/3 is included in Fig. 5 which clearly demonstrates that indeed, Eq. (8) holds very well in the region of thermodynamic stability of the liquid. Again we note that the agreement between THz-TDS, NMR, SED, and OHD-OKE can be taken as an additional piece of evidence that the long time tail of our Kerr-response is dictated by single-molecule diffusive reorientation. We also point out that, apparently, the values for τ_D

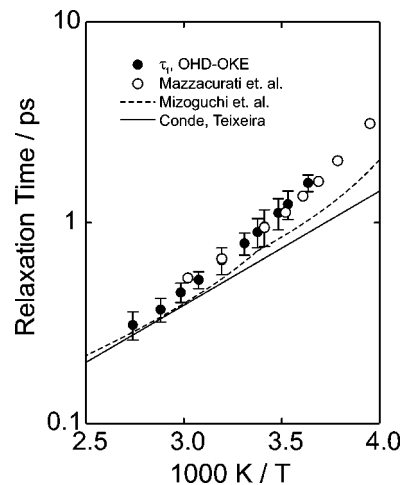


FIG. 6. Comparison of the time constant, τ_1 , characterizing the fast exponential component to the nuclear Kerr response of water (solid circles) with time constants obtained from depolarized Raman scattering. Open circles: time constants from Mazzacurati *et al.* (Ref. 19). Dashed curve: stepwise power-law dependence reported by Mizoguchi *et al.* Solid line: Arrhenius temperature dependence according to Conde and Teixeira (see Refs. 17 and 18).

extracted from THz-TDS data quantify the very same single molecule dynamics and not collective structural relaxations as previously suggested in Ref. 45. The same argument also holds for microwave data on the dielectric relaxation (DR) time published many years ago by Mason *et al.* (see Figs. 5 and Ref. 51).

D. Comparison with Raman scattering

So far, this discussion has focused only on the time constant characterizing the slow exponential due to single-molecule reorientation. As of today, neither time nor frequency-resolved Raman techniques have been able to record the full T -dependence of these dynamics.^{18,51} We believe that this could be due to sensitivity issues. The slow component has an amplitude which is almost two orders of magnitude smaller than that of the fast exponential. The latter, in turn, has an absolute Raman cross section of $\sim 2 \cdot 10^{-3} \text{ \AA}^6/\text{molecule}$ which amounts to less than 2% of the integrated intensity of the Brillouin doublet observed in high-resolution depolarized light scattering.¹⁹ Therefore, the slow component is likely to be masked in frequency-resolved spectra by leakage of the Brillouin peaks and spurious stray light. Note, however, that the OHD-OKE transients are not affected by elastic scattering. The rapid scan technique enhances the sensitivity of an optical Kerr-effect setup significantly (six decades of dynamic range, see Fig. 3) and allows this slow exponential tail to be revealed directly in the time-domain. Its extremely small intensity might also explain why such a narrow component has not been observed in molecular-dynamics simulations of the Raman response.^{6,7,12–14,52}

We now turn our attention to the fast exponential component of our OKE data. This “intermediate response” is obtained after subtracting the slow exponential discussed above from the raw Kerr-effect transients. The full temperature dependence of τ_1 is reproduced in Fig. 6 together with

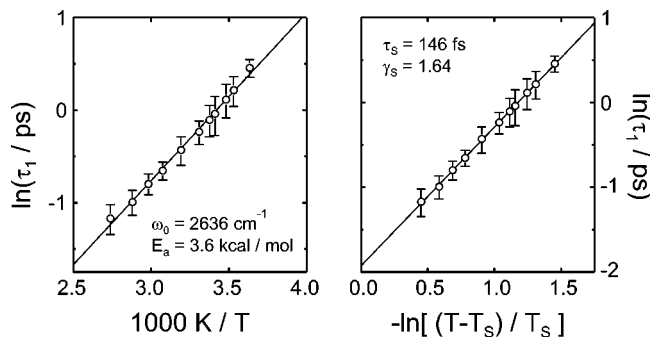


FIG. 7. Analysis of the temperature dependence of τ_1 . Open symbols: experimental data. Left panel: Least-squares fit according to an Arrhenius law yields $E_a = 3.6$ kcal/mol and $\omega_0 = 2636$ cm^{-1} . Right panel: Least-squares fit according to the Speedy–Angell relation yields $\tau_s = 146$ fs and $\gamma_s = 1.64$. The singular temperature was constrained to $T_s = 228$ K (see Ref. 3).

results from previous Raman scattering studies. Clearly, τ_1 is similar in magnitude to the time constants determined in the frequency domain. However, its detailed dependence on the temperature is markedly different.

According to Conde and Teixeira, the temperature dependence of this time constant is adequately represented by an Arrhenius law^{17,18}

$$\frac{\partial \ln \tau}{\partial 1/T} = \frac{E_a}{k_B}, \quad (9)$$

where E_a is the activation energy. A typical value for E_a of 2.6 kcal/mole with a corresponding pre-exponential factor, ω_0 , of 689 cm^{-1} was found.^{17,18} These results are reproduced in Fig. 6 by the solid line. The frequency deduced from the pre-factor lies within the broad librational band centered around 500 cm^{-1} . This result was interpreted with a thermally activated barrier crossing process which (necessarily) modulates the anisotropy of the polarizability. According to the pre-factor, crossing of this barrier is facilitated by motion along a librational (i.e., restricted rotational) coordinate.^{17,18} In addition, such an interpretation was consistent with a pronounced isotope effect on the pre-factor of roughly $\sqrt{2}$ similar to the isotopic shift of the librational band. Finally, a remarkable agreement of E_a with the activation energy reported by Walrafen,²² for breaking and formation of hydrogen bonds between water molecules, was found. Therefore, it was concluded that this time constant reflects a mean lifetime of hydrogen bonds in liquid water. Breaking of an H-bond is mediated by librational motion of the tetrahedrally coordinated water molecules with concurrent angular jumps of the proton across the tetrahedral angle once the O–H \cdots O bending angle exceeds a critical cut-off value.^{17,18}

From Fig. 6, it can be noticed that the fast exponential of the OKE data displays a much stronger temperature dependence as suggested by Eq. (9) using an activation energy and a pre-factor according to Ref. 18. Instead, applying an Arrhenius analysis to our data yields an activation energy, E_a , of 3.6 kcal/mole and a pre-factor, ω_0 , of 2636 cm^{-1} as shown in the left panel of Fig. 7. Especially the latter value is in stark contrast to the above mechanism of H-bond breakage and formation contributing to the intermediate exponential relaxation dynamics. It should also be pointed out that the

temperature range of thermodynamic stability of liquid water is very limited and proves insufficient for an accurate determination of the pre-factor through an extrapolation of the time constant to $1/T \rightarrow 0$. In particular, a reliable isotope effect on this quantity is very difficult to obtain.

Mizoguchi *et al.*, on the other hand, observed a rather complicated temperature dependence of the low-frequency Raman spectrum below 250 cm^{-1} .²⁰ In particular, they interpreted the central component with a Debye-type relaxation mode whose damping constant (or equivalently, inverse line width) followed a Curie–Weiss' law.²⁰ Such a temperature dependence emerges from the Speedy–Angell relation (3) by setting the critical exponent to unity. Below 298 K, a critical time constant of 229 fs and a singular temperature of 225 K were found, in good agreement with $T_s = 228$ K determined from compressibility data. However, for temperatures above 303 K, a better fit was obtained with $T_s = 251.5$ K and $\tau_s = 129$ fs.

The entire T -dependence as reported by Mizoguchi *et al.* is reproduced in Fig. 6 as the dashed curve. Again, it becomes clear, that our OKE data deviate from these Raman results especially near the melting point, where line width measurements become increasingly difficult. Near the boiling point, however, the central Lorentzian component becomes broader and, thus, its line width can be determined with higher accuracy. It is here, where OKE and depolarized Raman data converge.

The accuracy of line width measurements increases with enhanced frequency resolution. Using a single-mode Ar-ion-laser and a monochromator operating at a high diffraction order,⁹ Mazzacurati *et al.* were capable of detecting the central Raman component with a resolution of 0.046 cm^{-1} (as compared to 1.5 cm^{-1} in Ref. 20 and 1.2 cm^{-1} in Ref. 18). Their corresponding time constants are shown in Fig. 6 as open circles. In fact, an excellent agreement with our OHD-OKE data can be observed.

Following Mazzacurati *et al.*, this component is dominated by dipole–induced dipole interactions.¹⁹ In contrast to the fact that the number of water molecules participating to the hydrogen bond network is strongly temperature dependent, they found that the absolute Raman cross section for this component does not vary significantly upon heating the liquid. Therefore, they concluded that this feature cannot be related to the lifetime of hydrogen bonds. This conclusion was further substantiated by molecular dynamics simulations of the low-frequency Raman spectrum.⁵³ It was further noticed that the allowed rotational contribution to the spectrum (which includes the slow exponential decay of the OKE data) can only amount to about half the intensity of the central Raman component.¹⁹ By analyzing their line widths according to the Speedy–Angell relation (3), Mazzacurati *et al.* suggested that the polarizability fluctuations responsible for the central component is related to the same degrees of freedom which determine the bulk thermodynamic and transport properties of the liquid.¹⁹

The Speedy–Angell relation with the singular temperature being fixed at 228 K (see Ref. 3) is applied to the OKE time constants, τ_1 , in the right panel of Fig. 7. Least-squares fitting yields $\gamma_s = 1.65$ and $\tau_s = 146$ fs. We point out, how-

ever, that the investigated temperature range is too limited to distinguish between a power law or Arrhenius law dependence. Yet, based on the arguments given above and considering the fitting parameter obtained from Eq. (9), an Arrhenius-type temperature dependence of τ_1 seems highly unlikely.

The frequency derived from the critical time constant of the Speedy–Angell fit is located in the region of the high-frequency restricted translational mode. According to Walrafen, the mechanical origin of the restricted translational modes of the liquid can be traced back to solidlike local vibrations of translational character. Their frequencies agree rather well with the zone-edge transverse acoustic (TA) and longitudinal acoustic (LA) phonon frequencies of amorphous and crystalline ice (i.e., 65–70 cm^{-1} for TA and 164–181 for LA). The latter is modulating the density-related next-nearest neighbor O–O distance. In analogy to Ref. 4, one might conclude that fluctuations in the H-bond stretching vibrations are also involved in driving the anomalous density fluctuations near T_S . Such an interpretation is also consistent with the dilational character of a solidlike LA-phonon which must modulate a density related distance in the liquid.²¹ Higher order (delocalized), restricted translational modes involving motion of neighboring O–O units may be responsible for the fast exponential observed in our OHD-OKE data since their dynamics are likely to be in the overdamped limit. Further experiments including studies on the isotope effect are currently in progress in our group to test this microscopic picture in more detail.

V. CONCLUSIONS

In summary, we have performed detailed experiments on the temperature dependence of the long-time tail of the nuclear Kerr response in water. The high dynamic range of our data made it possible to identify two exponential contributions on longer delays. A detailed comparison with nuclear magnetic resonance and THz time domain spectroscopy strongly suggests that the slower exponential component is due to the diffusive single-molecule rotational motion of the water molecules and not, as is commonly observed for non-hydrogen bonded liquids, due to collective reorientation. The fact that these dynamics have not been observed in previous OHD-OKE studies is due to an almost isotropic optical anisotropy of the water molecules which makes their Raman spectroscopic detection extremely difficult.⁵⁴ Furthermore, single-molecule reorientational dynamics in this highly structured liquid are described surprisingly well by the Stokes–Einstein–Debye equation.

Previous OHD-OKE studies have mistakenly assigned the fast exponential contribution to rotational diffusion of the water molecules and have led to much confusion with respect to the convergence of apparently distinct but intimately related spectroscopic techniques for probing liquid dynamics. Instead, we find that this “intermediate response” is in qualitative agreement with frequency-domain depolarized Raman scattering. Although the temperature range accessible in our present OHD-OKE setup is rather limited, it seems highly unlikely that the time constant of this fast exponential follows an Arrhenius behavior. An analysis employing the

Speedy–Angell relation, which is known to describe a great number of static and dynamic properties of water very well, suggests that the intermediate response is linked to overdamped restricted translational modes in the strongly hydrogen bonded liquid network.

Isotope studies are currently underway in our laboratories to further investigate the connection of these intermediate dynamics to the optic and acoustic degrees of freedom of the liquid.

ACKNOWLEDGMENTS

Financial support by the Deutsche Forschungsgemeinschaft through the Sonderforschungsbereich SFB 357 “Molekulare Mechanismen unimolekularer Reaktionen” is gratefully acknowledged.

- ¹*The Physics and Physical Chemistry of Water, Vol. 1*, edited by F. Franks (Plenum, New York, 1972).
- ²D. Eisenberg and W. Kauzmann, *The Structure and the Properties of Water* (Oxford University Press, Oxford, 1969).
- ³C. A. Angell, *Annu. Rev. Phys. Chem.* **34**, 593 (1983).
- ⁴E. W. Lang and H.-D. Lüdemann, *Angew. Chem. Int. Ed. Engl.* **21**, 315 (1982).
- ⁵F. H. Stillinger and A. Rahman, *J. Chem. Phys.* **60**, 1545 (1974).
- ⁶R. W. Impey, P. A. Madden, and I. R. McDonald, *Mol. Phys.* **46**, 513 (1982).
- ⁷P. A. Madden and R. W. Impey, *Chem. Phys. Lett.* **123**, 502 (1986).
- ⁸M. A. Ricci, G. Ruocco, and M. Sampoli, *Mol. Phys.* **67**, 19 (1989).
- ⁹W. Bosma, L. E. Fried, and S. Mukamel, *J. Chem. Phys.* **98**, 4413 (1992).
- ¹⁰M. Cho, G. R. Fleming, S. Saito, I. Ohmine, and R. M. Stratt, *J. Chem. Phys.* **100**, 6672 (1994).
- ¹¹S. Sastry, H. E. Stanley, and F. Sciortino, *J. Chem. Phys.* **100**, 5361 (1994).
- ¹²S. Saito and I. Ohmine, *J. Chem. Phys.* **106**, 4889 (1997).
- ¹³I. Ohmine and S. Saito, *Acc. Chem. Res.* **32**, 741 (1999).
- ¹⁴B. D. Bursulaya and H. J. Kim, *J. Chem. Phys.* **109**, 4911 (1998).
- ¹⁵P. L. Silvestrelli, M. Bernasconi, and M. Parrinello, *Chem. Phys. Lett.* **277**, 478 (1997).
- ¹⁶P. L. Silvestrelli and M. Parrinello, *J. Chem. Phys.* **111**, 3572 (1999).
- ¹⁷O. Conde and J. Teixeira, *Mol. Phys.* **53**, 951 (1984).
- ¹⁸O. Conde and J. Teixeira, *J. Phys. (France)* **44**, 525 (1983).
- ¹⁹V. Mazzacurati, A. Nucara, M. A. Ricci, G. Ruocco, and G. Signorelli, *J. Chem. Phys.* **93**, 7767 (1990).
- ²⁰K. Mizoguchi, Y. Hori, and Y. Tominaga, *J. Chem. Phys.* **97**, 1961 (1992).
- ²¹G. E. Walrafen, *J. Phys. Chem.* **94**, 2237 (1990).
- ²²G. E. Walrafen, M. R. Fisher, M. S. Hokmabadi, and W.-H. Yang, *J. Chem. Phys.* **85**, 6970 (1986).
- ²³G. E. Walrafen, M. S. Hokmabadi, W.-H. Yang, Y. C. Chu, and B. Monosmith, *J. Phys. Chem.* **93**, 2909 (1989).
- ²⁴S. Krishnamurthy, R. Bansil, and J. Wiafe-Akenten, *J. Chem. Phys.* **79**, 5863 (1983).
- ²⁵M. Cho, M. Du, N. F. Scherer, G. R. Fleming, and S. Mukamel, *J. Chem. Phys.* **99**, 2410 (1993).
- ²⁶C. Kalpouzos, W. T. Lotshaw, D. McMorro, and G. A. Kennedy-Wallace, *J. Phys. Chem.* **91**, 2028 (1987).
- ²⁷W. T. Lotshaw, D. McMorro, C. Kalpouzos, and G. A. Kenney-Wallace, *Chem. Phys. Lett.* **136**, 323 (1987).
- ²⁸D. McMorro, W. T. Lotshaw, and G. A. Kenney-Wallace, *IEEE J. Quantum Electron.* **24**, 443 (1988).
- ²⁹P. Cong, H. P. Deuel, and J. D. Simon, *Chem. Phys. Lett.* **240**, 72 (1995).
- ³⁰Y. J. Chang and E. W. Castner, *J. Phys. Chem.* **100**, 3330 (1996).
- ³¹B. J. Loughnane, A. Scodinu, R. A. Farrer, J. T. Fourkas, and U. Mohanty, *J. Chem. Phys.* **111**, 2686 (1999).
- ³²E. W. Castner, Y. J. Chang, Y. C. Chu, and G. E. Walrafen, *J. Chem. Phys.* **102**, 653 (1995).
- ³³S. Palese, S. Mukamel, R. J. D. Miller, and W. T. Lotshaw, *J. Phys. Chem.* **100**, 10380 (1996).
- ³⁴S. Palese, L. Schilling, R. J. D. Miller, P. R. Staver, and W. T. Lotshaw, *J. Phys. Chem.* **98**, 6308 (1994).

- ³⁵Y. J. Chang and E. W. J. Castner, *J. Chem. Phys.* **99**, 7289 (1993).
- ³⁶M. J. Feldstein, P. Vöhringer, and N. F. Scherer, *J. Opt. Soc. Am. B* **12**, 1500 (1995).
- ³⁷E. Lang and H.-D. Lüdemann, *J. Chem. Phys.* **67**, 718 (1977).
- ³⁸E. Lang and H.-D. Lüdemann, *Ber. Bunsenges. Phys. Chem.* **84**, 462 (1980).
- ³⁹E. W. Lang and H.-D. Lüdemann, *Ber. Bunsenges. Phys. Chem.* **85**, 603 (1981).
- ⁴⁰G. Sposito, *J. Chem. Phys.* **74**, 6943 (1981).
- ⁴¹L. Thrane, R. H. Jacobsen, P. U. Jepsen, and S. R. Keiding, *Chem. Phys. Lett.* **240**, 330 (1995).
- ⁴²B. N. Flanders, R. A. Cheville, D. Grischkowsky, and N. F. Scherer, *J. Phys. Chem.* **100**, 11824 (1996).
- ⁴³J. T. Kindt and C. A. Schmuttenmaer, *J. Chem. Phys.* **106**, 4389 (1997).
- ⁴⁴S. R. Keiding, *J. Phys. Chem.* **101**, 5250 (1997).
- ⁴⁵C. Rønne, P.-O. Åstrand, and S. R. Keiding, *Phys. Rev. Lett.* **82**, 2888 (1999).
- ⁴⁶C. Rønne, P.-O. Åstrand, A. Wallqvist, K. V. Millelson, and S. R. Keiding, *J. Chem. Phys.* **107**, 5319 (1997).
- ⁴⁷H. Harde, N. Katzenellenbogen, and D. Grischkowsky, *Phys. Rev. Lett.* **74**, 1307 (1995).
- ⁴⁸R. M. Lynden-Bell and I. R. McDonald, *Mol. Phys.* **43**, 1429 (1981).
- ⁴⁹R. M. Lynden-Bell and I. R. McDonald, *Chem. Phys. Lett.* **89**, 105 (1982).
- ⁵⁰R. M. Lynden-Bell and W. A. Steele, *J. Phys. Chem.* **88**, 6514 (1984).
- ⁵¹P. R. Mason, J. B. Hasted, and L. Moore, *Adv. Mol. Relax. Processes* **6**, 217 (1974).
- ⁵²B. D. Bursulaya and H. J. Kim, *J. Phys. Chem. B* **101**, 10994 (1997).
- ⁵³V. Mazzacurati, M. A. Ricci, G. Ruocco, and M. Sampoli, *Chem. Phys. Lett.* **159**, 383 (1989).
- ⁵⁴W. H. Orttung and J. A. Meyers, *J. Phys. Chem. Ithaca* **67**, 1905 (1963).